Early Evolution of Rotating Star Clusters

A. L. Varri[1,2], E. Vesperini[2], M. Tiongco[2], S. L. W. McMillan[3], C. M. Gosmeyer[4]

[1] University of Edinburgh (UK) [2] Indiana University (USA) [3] Drexel University (USA) [4] Space Telescope Science Institute (USA)

Outline

- An increasing number of star clusters are being observed to have significant evidence of internal rotation. In this respect, it is crucial to understand the role of angular momentum during the initial stages of star cluster dynamical evolution.
- Driven by this motivation, we explored the dynamics of dissipationless collapse in the presence of non-vanishing initial total angular momentum.
- We present here the preliminary results of an extended survey of N-body simulations starting from homogeneous and inhomogeneous initial density distributions with different amounts of total angular momentum and pressure support.

Evidence of internal rotation in star clusters

New high precision spectroscopic observations and HST proper motion studies of thousands of stars in selected Galactic globular clusters are beginning to reveal detailed information about the three-dimensional kinematics of this class of stellar systems. Such a complete view of their velocity space calls for more realistic dynamical modeling, in which the effects of internal rotation are fully taken into account.

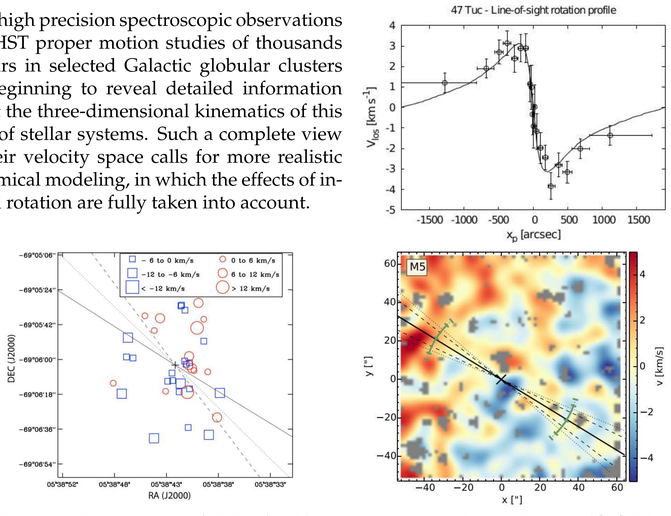

Fig. 1: Top panel: Rotation curve of 47 Tuc, fitted by an axisymmetric rotating VB12 model [16] (taken from [3]). **Bottom left panel:** Schematic view of the velocity field of the young massive star cluster R136 from the VLT-FLAMES Tarantula Survey, solid line denotes the optimal rotation axis (taken from [10]). **Bottom right panel:** Velocity field of M5 from the IFU instrument VIRUS-W; solid line denotes the kinematic PA, green arcs the photometric PA. (taken from [7]).

Method and initial conditions

We designed a survey of N-body simulations to investigate the effects of non-vanishing total angular momentum on the dynamics of dissipationless collapse (see also [9][11][1][8][4]). The initial configurations are characterized by homogeneous and inhomogeneous density distributions and uniform rotation, with different values of $Q_{rot} = 2K_{rot}/|W|$ and $Q_{ran} = 2K_{ran}/|W|$, where K and W denote the kinetic and potential energy, respectively. All models ($N = 65536$ equal-mass particles) have been followed during the collapse phase, until the configurations have reached equilibrium conditions (typically, at least $T = 20$ N-body units). All simulations have been performed with `starlab` [13].

Q_{rot} \ Q_{ran}	**0.10**	**0.25**	**0.5**	**0.75**
0.00	H1a	H1b	H1c	H1d
0.16	H2a	H2b	H2c	H2d
0.33	H3a	H3b	H3c	H3d
0.50	H4a	H4b	H4c	H4d

Q_{rot} \ Q_{ran}	**0.10**	**0.25**	**0.1**	**0.25**
0.00	F28_1a	F28_1b	F24_1a	F24_1b
0.16	F28_2a	F28_2b	F24_2a	F24_2b
0.33	F28_3a	F28_3b	F24_3a	F24_3b
0.50	F28_4a	F28_4b	F24_4a	F24_4b

Tab. 1 (left): Properties of the homogeneous (H) initial conditions. The degree of rotation increases from 1 (non-rotating) to 4; the pressure support increases from a (cold) to d (warm). **Tab. 2 (right):** Properties of the inhomogeneous initial conditions. The initial (non-rotating) configurations have been generated by using `MCluster` [12], with fractal dimensions $D = 2.8$ (F28, moderate deviations from homogeneity) $D = 2.4$ (F24, significant deviations from homogeneity).

Morphological evolution

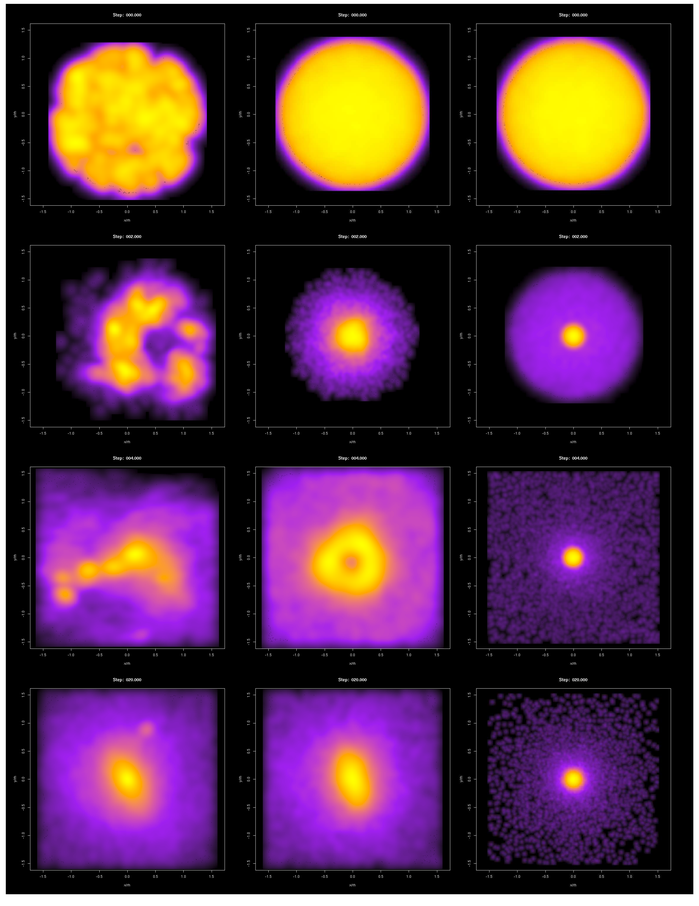

Fig. 2: Time evolution of the surface density of models (left to right column) **F24_3a (clumpy, cold, rotating)**, **H3a (homogeneous, cold, rotating)**, and **H1a (homogeneous, cold, non-rotating)** projected on the equatorial plane (x, y). The systems are evaluated at $T = 0, 2, 4, 20$ N-body time units (top to bottom row). The spatial coordinates are scaled with respect to the initial half-mass radius. Although characterized by the same initial value of Q_{ran}, the depth of the collapse experienced by the models is significantly affected by the presence of rotation and clumpiness. Note also that some rapidly rotating models in our survey may be dynamically unstable with respect to bar modes (e.g., see the bottom left panels).

A glimpse of the phase space

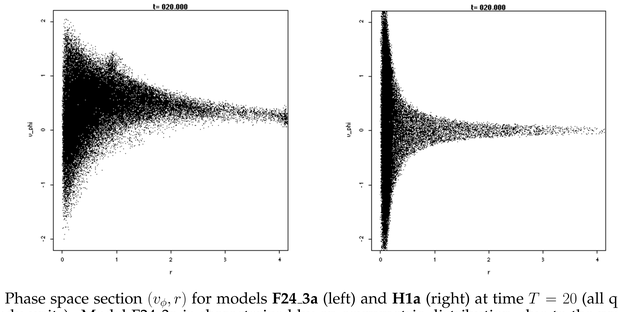

Fig. 3: Phase space section (v_ϕ, r) for models **F24_3a** (left) and **H1a** (right) at time $T = 20$ (all quantities in N-body units). Model F24_3a is characterized by an asymmetric distribution, due to the presence of rotation, and by few long-lived substructures. Model H1a shows a clear core-halo structure.

Rotation and Anisotropy

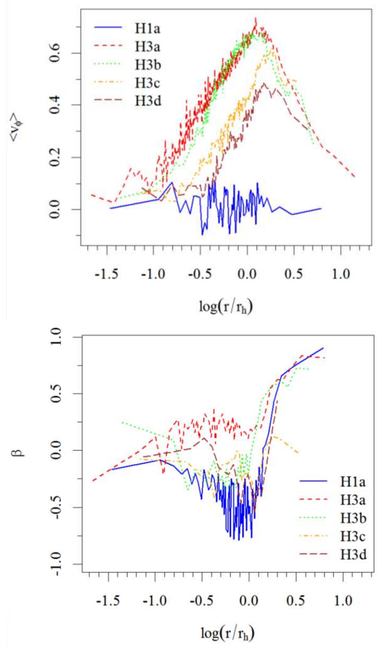

Kinematical properties at $T = 20$ of a selection of models starting from homogeneous initial conditions, characterized by the same initial value of Q_{rot}, but different values of Q_{ran} (to be compared with the non-rotating model H1a). The profiles have been constructed by considering thin cylindrical rings on the equatorial plane, with equal number of particles.

Fig. 4 (top): Rotation curves. During the collapse, the distribution of angular momentum evolves from uniform to differential rotation, with a profile characterized by approximately constant angular velocity in the inner regions and a peak around the half-mass radius.

Fig. 5 (bottom): Radial profiles of the anisotropy parameter $\beta = 1 - (\sigma_\theta^2 + \sigma_\phi^2)/2\sigma_r^2$. As expected from previous numerical experiments of violent relaxation with non-rotating initial conditions [14][5], the outer parts of the models are characterized by radial anisotropy. Interestingly, some systems are characterized by tangential anisotropy in the intermediate regions (see also [15]). This kinematical signature may be relevant in the dynamical interpretation of some peculiar phase space properties of dwarf spheroidal galaxies, such as Sculptor (e.g., see [5]).

Density slope - Anisotropy relation

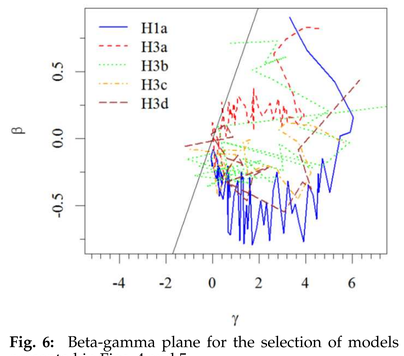

Fig. 6: Beta-gamma plane for the selection of models presented in Figs. 4 and 5.

Recently, it has been demonstrated [2] [6] that in an anisotropic spherical stellar system the density profile slope γ is related to the anisotropy β by the inequality

$$\beta \leq \gamma/2\,. \qquad (1)$$

The configurations considered in our study are consistent with this relation. We wish to emphasize that this is one of the first examples in which this inequality has been shown to hold also for non-spherical rotating (tangentially-biased) stellar systems.

ALV thanks D. C. Heggie for discussions and acknowledges support from the Royal Commission for the Exhibition of 1851 and The Gruber Foundation.

Questions?
annalisa.varri@gmail.com
@parallasseh
http://alvarri.com

References

[1] Aguilar, L. A., & Merritt, D. 1990, ApJ, 354, 33
[2] An, J. H., & Evans, N. W. 2006, ApJ, 642, 752
[3] Bianchini, P., Varri, A. L., et al. 2013, ApJ, 772, 67
[4] Boily, C.M, & Athanassoula, E. 2006, MNRAS, 369
[5] Breddels, M. A., et al. 2013, MNRAS, 433, 3173
[6] Ciotti, L., & Morganti, L. 2010, MNRAS, 408, 1070
[7] Fabricius, M., Noyola, E., et al. 2014, ApJL, 787, L26
[8] Goodwin, S., & Whitworth, A. 2003, A&A, 413, 929
[9] Gott, R. J. 1973, ApJ, 186, 481
[10] Hénault-Brunet, V., et al. 2012, A&A, 545, L1
[11] Hohl, F., & Zang, T. A. 1979, AJ, 84, 585
[12] Küpper, A. H. W. et al . 2011, MNRAS, 417, 2300
[13] Portegies Zwart, S. F., et al. 2001, MNRAS, 321, 199
[14] van Albada, T. S., 1982, MNRAS, 201, 939
[15] Trenti, M., Bertin, G., et al., 2005, A&A, 433, 57
[16] Varri, A. L., & Bertin, G. 2012, A&A, 540 (VB12)